Inorganic Chemistry

Article

pubs.acs.org/IC

Pressure-Dependent Enhanced T_c and Magnetic Behavior of the Metamagnetic and Ferromagnetic Polymorphs of $[Fe^{III}Cp^*_2]^{\bullet+}[TCNQ]^{\bullet-}$ (Cp* = Pentamethylcyclopentadienide; TCNQ = 7,7,8,8-Tetracyano-*p*-quinodimethane)

Jack G. DaSilva and Joel S. Miller*

Department of Chemistry, 315 S 1400 East, University of Utah, Salt Lake City, Utah 84112-0850, United States

ABSTRACT: The magnetic behaviors of the metamagnetic and ferromagnetic polymorphs of $[Fe^{III}Cp_2^*]^{\bullet+}[TCNQ]^{\bullet-}$ (Cp* = pentamethylcyclopentadienide; TCNQ = 7,7,8,8-tetracyano-*p*-quinodimethane) were studied as a function of hydrostatic pressure. Both polymorphs exhibit a reversible enhancement of magnetic properties with increasing pressure. The T_c for the ferromagnetic polymorph increased by 70% from 2.95 to 5.01 K at 10.3 kbar at a rate of 0.21 K/kbar, which is similar to the 0.22 K/kbar reported for $[FeCp_2^*]^+[TCNE]^-$. The coercive field and remnant magnetization exhibit exponential-like growth upon application of external pressure, increasing from zero at ambient pressure to 550 Oe and 8880 emu·Oe/mol at 10.3 kbar, respectively. The T_c for the metamagnetic polymorph was determined to be 2.10 K from the maximum in the Fisher specific heat data, that is, $d(\chi T)/dT$, and it increases by 38% to 2.90 K at 2.9 kbar at a rate of 0.28 K/kbar, before vanishing, in accord with a transition to a paramagnetic state. The metamagnetic critical field, H_c, determined from dM/dH increases linearly from 1300 Oe at ambient pressure to 1800 Oe at 2.9 kbar, but is not evident at and above 3.9 kbar, also in accord with a transition to a paramagnetic state.

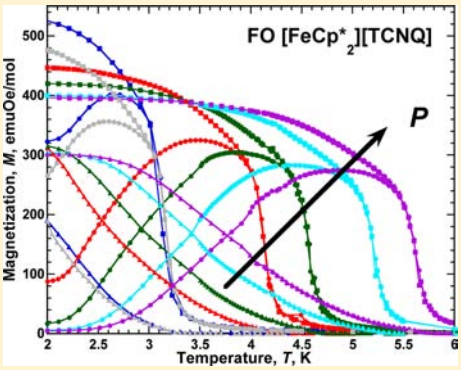

INTRODUCTION

The $[Fe^{III}Cp_2^*]^{\bullet+}[TCNQ]^{\bullet-}$ (Cp* = pentamethylcyclopentadienide; TCNQ = 7,7,8,8-tetracyano-*p*-quinodimethane) electron-transfer salt was first synthesized in an attempt to create an organic-based conductor.[1] While not an organic-based metal, $[FeCp_2^*]^+[TCNQ]^-$ exhibited metamagnetic behavior.[2] This led to the synthesis of $[FeCp_2^*]^+[TCNE]^-$ (TCNE = tetracyanoethylene) as the first organic-based ferromagnet,[3−5] and subsequently the first organic-based room-temperature magnet, $V[TCNE]_x$,[6,7] and evidence of their suitability for the discovery of multifunctional materials.[8]

$[Fe^{III}Cp_2^*]^+[TCNQ]^-$ is an electron-transfer salt resulting from the reaction of TCNQ and $Fe^{II}Cp_2^*$ that crystallizes into three structurally and magnetically 1:1 distinct phases, namely,[5] paramagnetic,[9,10] metamagnetic (**MM**),[10] and ferromagnetic (**FO**) polymorphs.[11] The **MM** and **FO** polymorphs have the same structural motif of chains of alternating cations, $[FeCp_2^*]^+$, and anions, $[TCNQ]^-$. However, the 1-D chains in the **MM** phase possess $[TCNQ]^-$ planes that are approximately parallel to the plane of the Cp* ring, the centroids of both lie along the chain axis, and both planes are approximately orthogonal to the chain axis.[10] In contrast, the chains in the **FO** phase have the $[TCNQ]^-$ planes approximately parallel to the plane of the Cp* ring, the centroids are not aligned, and the planes of both are not orthogonal to the chain axis.[11]

The pentamethylcyclopentadienide ligand exerts a strong crystal field, causing the Fe^{III} to be low-spin. Thus, $S = 1/2$ $[FeCp_2^*]^+$ couples with the $S = 1/2$ $[TCNQ]^-$. A computational investigation of the similarly structured $[FeCp_2^*]^+[TCNE]^-$ indicates that the magnetic behavior arises from strong intrachain coupling and weak interchain coupling (2 orders of magnitude smaller).[12] Thus, although the inter- and intrachain interactions are necessary for magnetic order, the paramagnetic behavior above the ordering temperature, T_c, is appropriately modeled as 1-D chains.[13]

Ferromagnetic $[FeCp_2^*][TCNQ]$ (**FO**) has a magnetic ordering temperature, T_c, of 3.1 K from the maximum in the frequency-independent $\chi'(T)$ data and 3.0 K from the maximum in the specific heat, $C_p(T)$, data, and a saturation magnetization of 16 740 emu·Oe/mol,[14] but it does not exhibit hysteresis at 2 K.[15] Aligned crystals of metamagnetic $[FeCp_2^*][TCNQ]$ (**MM**) saturate at 15 900 emu·Oe/mol, and have a 1300 Oe critical field, H_c, at 2 K that decreases with increasing temperature. The T_c is 2.5 K from the maximum in the frequency-independent $\chi'(T)$ data, and peak maximum in $C_p(T)$ data.[14]

The 0-D structural isolated-ion nature of $[FeCp_2^*]^+[TCNQ]^-$ suggests that application of hydrostatic pressure may lead to enhanced intra- and interchain couplings,

Received: November 6, 2012
Published: December 26, 2012

   dx.doi.org/10.1021/ic302420s | *Inorg. Chem.* 2013, 52, 1108−1112

and a higher magnetic ordering temperature, T_c, as observed for $[FeCp_2^*]^+[TCNE]^-$,[16] and $[FeCp_2^*]^+[DCNQ]^-$ (DCNQ = 2,3-dicyano-1,4-naphthoquinone).[17] Herein, we report the pressure dependence of magnetism for **MM** and **FO** due to their structural and electrochemical similarities to $[FeCp_2^*]^+[TCNE]^-$.

EXPERIMENTAL SECTION

FO and **MM** were prepared via the literature methods.[14] IR spectroscopy and AC susceptibility were used to confirm purity. IR spectra were measured from 400 to 4000 cm^{-1} using a Bruker Tensor 37 spectrometer (±1 cm^{-1}). A Quantum Design (QD) Physical Property Measurement System PPMS 9 T was used to measure the AC susceptibility at ambient pressure. Samples of **FO** and **MM** (3−15 mg) were loaded into gelatin capsules in an inert atmosphere and sealed with silicone grease prior to removal from the inert atmosphere. A QD superconducting quantum interference device (SQUID) Magnetic Property Measurement System (MPMS-5XL 5 T) (sensitivity = 10^{-8} emu or 10^{-12} emu/Oe at 1 T) was used to perform the DC pressure-dependent magnetization studies. Samples of **FO** and **MM** (~1 mg) were sealed into a cylindrical Teflon cell; the remaining volume of the cell was occupied by decalin (the hydrostatic pressure media) and capped with Teflon end caps. The loaded Teflon sample cell was housed in a beryllium−copper hydrostatic pressure cell, fabricated at the University of Utah from the Kyowa Seisakusho design, with zirconia pistons and rubber o-rings. Pressure was applied to the assembly using a Kyowa Seisakusho CR-PSC-KY05-1 apparatus with a WG-KY03-3 pressure sensor. An Aikoh Engineering model-0218B digital sensor readout was used as the pressure indicator. For the zero-field-cooled magnetization, $M_{ZFC}(T)$, the sample was cooled in zero applied field, and the data were taken upon warming in a 5 Oe applied field, whereas, for the field-cooled magnetization, $M_{FC}(T)$, the sample was cooled in a 5 Oe applied field, and the data were taken upon warming in a 5 Oe applied field. The remnant magnetization, $M_r(T)$, was taken upon warming in a zero applied field after the sample was cooled in a 5 Oe applied field.

The Aikoh Engineering model-0218B digital sensor readout is an approximate method for determining pressure, and a superconductor with a known pressure-dependent transition temperature, $T_{sc}(P)$, for example, Pb,[18] was used to calibrate the pressure. Since the expected T_{sc} for both **MM** and **FO** is in the range of 2−4 K,[14] no convenient superconducting pressure calibrant with a lower T_{sc} was available. Nonetheless, a statistical analysis of 159 individual pressure applications (Figure 1) from several previous studies using the identical digital sensor readout, and using a superconducting pressure calibrant, enabled the determination of the pressure, P, in kbar, from a least-squares linear regression fit (eq 1), where x is the readout from the digital sensor. The error associated with this correlated fit was assumed to be twice the standard deviation, 2σ, of 0.83 kbar. The data were collected over several years to remove any technique-based bias, and χ^2 is 0.95301. As pointed out by a reviewer, the pressure dependence is never the same due to the difference in volume, tightness of the joints, etc., and this accounts for the scatter of the data.

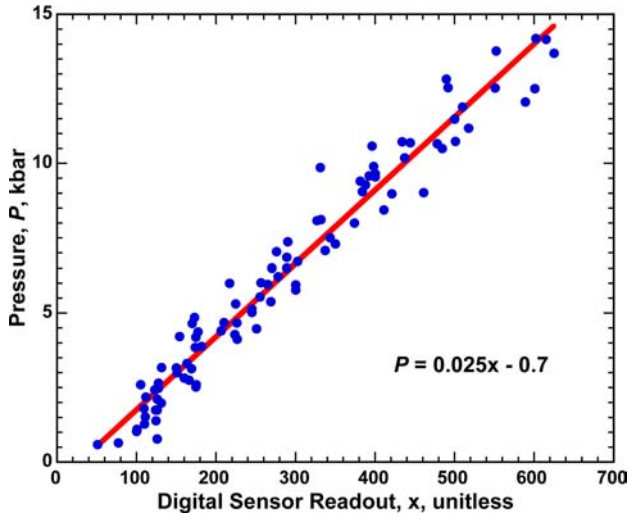

Figure 1. Correlation of 159 calibrated pressures (●) as a function of the digital sensor readout, x. The red line is the least-squares linear regression fit (eq 1).

$$P = 0.025x - 0.7 \quad (1)$$

The T_c of **FO** was determined through the extrapolation of the most linear portion of the remnant magnetization, $M_r(T)$, near zero magnetization to zero magnetization. The bifurcation temperature was taken as the temperature at which the divergence of zero-field-cooled, $M_{ZFC}(T)$, and field-cooled, $M_{FC}(T)$, magnetizations occur. The T_c of **MM** was determined from the maximum in the $d(\chi T)/dT$, that is, the Fisher specific heat.[19,20] Isothermal field-dependent magnetization measurements, $M(H)$, were performed for both phases at 2 K, and the coercive field, H_{cr}, of **FO** was determined from the extrapolation of the field intercept at zero magnetization upon reduction of an applied field of ±50 kOe. The $M_r(H)$ for **FO** was determined from the extrapolation of the magnetization intercept at zero applied field upon reduction of an applied field of ±50 kOe, and the critical field, H_c, of **MM** was defined as the maximum in dM/dH of the virgin curve.

RESULTS AND DISCUSSION

The pressure-dependent magnetization as a function of applied field, $M(H,P)$, at 2 K, as well as the remnant magnetization, $M_r(T,P)$, zero-field-cooled and field-cooled magnetizations, $M_{ZFC}(T,P)$ and $M_{FC}(T,P)$, for **FO**, and as a function of applied field, $M(H,P)$ at 2 K, as a function of temperature at 500 Oe for **MM** were measured.

The **FO** polymorph of $[FeCp^*_2][TCNQ]$ was previously analyzed through AC and DC magnetometry and was found to have a T_c(AC) [from the maximum in $\chi'(T)$] of 3.1 K, a $T_c(M_{FC}(T))$ [from the extrapolation of the most linear portion of $M_{FC}(T)$ to zero magnetization] of 3.0 K, a $T_c(M_r(T))$ [from the extrapolation of the most linear portion of $M_r(T)$ to zero magnetization] of 3.3 K, a bifurcation temperature, T_b [from the divergence of the $M_{ZFC}(T)$ and $M_{FC}(T)$ magnetizations] of 3.0 K, and no coercive field, H_{cr}.[11,15] These values were reproduced through similar measurements at ambient pressure: $T_c(M_r(T)) = 2.95 \pm 0.05$ K, $T_b = 2.92 \pm 0.05$ K, and coercivity, H_{cr}, of 0 ± 2.5 Oe. The H_{cr} is consistent with an initial report of no coercivity, and within the sensitivity of measurements is zero.[11] Polycrystalline samples were used to be consistent with those used in the pressure cell.

The $M_r(T)$, $M_{ZFC}(T)$, and $M_{FC}(T)$ for **FO** decrease with increasing applied pressure by ~25% at 10.3 kbar (Figure 2). The rate of the magnetization suppression approaches zero above 7.7 kbar, which is most apparent in the low-temperature region of the $M_{FC}(T)$ data (Figure 2). The $T_c(M_r(T))$ and T_b increase by 0.21 and 0.25 K/kbar, respectively (Figure 2), which are similar to the reported trend from AC measurements of T_c for $[FeCp_2^*]^+[TCNE]^-$ of 0.22 K/kbar.[16] The $T_c(M_r(T))$ and T_b increased by 70 and 87% from 2.95 and 2.92 K at ambient pressure to 5.01 and 5.46 K, respectively, at 10.3 kbar (Figure 3).

The magnetization at 50 kOe was somewhat reduced from 12 900 emu·Oe/mol at ambient pressure to 11 000 emu·Oe/mol at 10.3 kbar (Figure 4), in accord with that observed in the $M_r(T)$, $M_{ZFC}(T)$, and $M_{FC}(T)$ data. The H_{cr} and $M_r(P)$ exhibit exponential-like growth upon application of an external pressure, increasing from zero at ambient pressure to 550 Oe

dx.doi.org/10.1021/ic302420s | Inorg. Chem. 2013, 52, 1108−1112

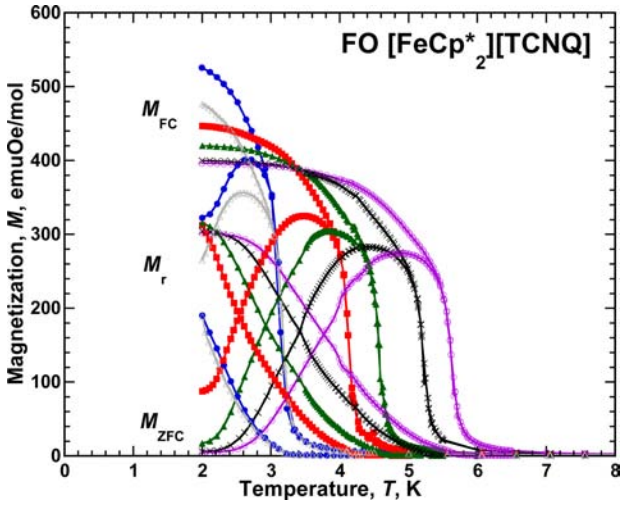

Figure 2. $M_r(T)$, $M_{ZFC}(T)$, and $M_{FC}(T)$ of **FO** at 0.001 (●) (ambient pressure), 3.3 (■), 5.2 (▲), 7.7 (×), and 10.3 kbar (○), and upon returning to ambient pressure [0.001 kbar (△)]. The lines are guides for the eye.

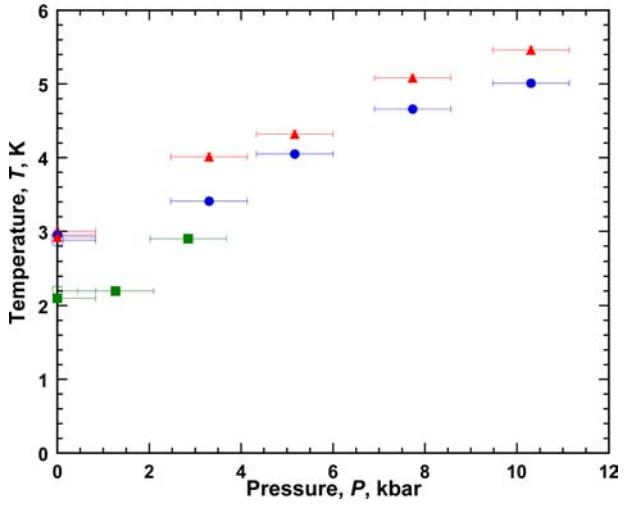

Figure 3. T_c(●) [from $M_r(T)$] and T_b(▲) of **FO**, and T_c (■) [from the temperature at which $d(\chi T)/dT$ is maximum] for **MM** as a function of pressure. Data for the released pressure measurements are hollow symbols (Δ, o, □). Error bars for temperature are less than the size of the symbol.

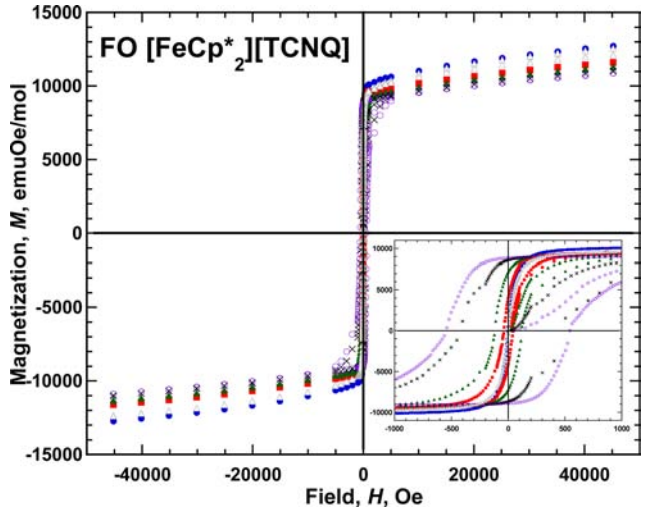

Figure 4. $M(H)$ of **FO** at ambient pressure, 0.001 (●), and 3.3 (■), 5.2 (▲), 7.7 (×), and 10.3 kbar (○), and upon returning to ambient pressure [0.001 kbar (△)]. Inset is an expansion of the hysteretic behavior.

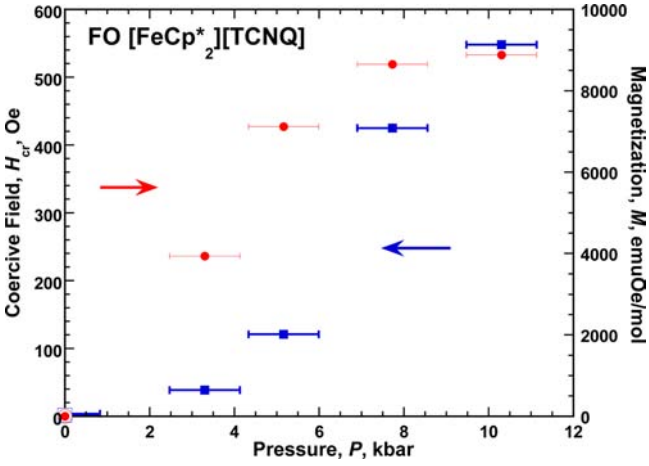

Figure 5. $H_{cr}(P)$ (■) and $M_r(P)$ (●) of **FO**; the released pressure measurements are hollow symbols (o, □). Error bars for H_{cr} and M_r are less than the size of the symbol.

and 8880 emu·Oe/mol at 10.3 kbar, respectively (Figure 5). The $M_r(H)$ approaches a constant value at ~7.7 kbar, while the rate of improvement in the H_{cr} decreases, which may indicate that the T_c has risen sufficiently above 2 K (the hysteresis measurement temperature) to prevent thermal disruption of the hysteresis as in the behavior of H_c in metamagnets.[21] The T_c, T_b, and H_{cr} were restored to their ambient pressure values, 2.88 ± 0.05 K, 3.00 ± 0.05 K, and 0 ± 2.5 Oe, respectively, upon returning to ambient pressure, indicating reversibility of the magnetic properties.

Under hydrostatic pressure, the intra- and interchain separations contract, leading to stronger couplings enhancing T_c and the bifurcation temperature, T_b. The increase in the magnetic irreversibility as evidenced by the appearance and growth of H_c and, consequently, the M_r is more complex, as the lack of the coercivity at ambient pressure is at variance with the 1 kOe coercivity for [$FeCp_2$*][TCNE] at 2 K at ambient pressure.[7,13] A theoretical analysis in conjunction with a study of the pressure-dependent structure is needed to understand the genesis of these effects.

MM has been extensively studied through AC, and, to a lesser extent, DC magnetometry and was found to have a T_c [from the maximum in $\chi'(T)$] of 2.6 K,[14] T_c [from the maximum in $\chi(T)$] of 2.55 K,[214] and a critical field, H_c [from the maximum in dM/dH] of 1300 Oe at 2 K.[14] These values were reproduced at ambient pressure: $T_c[\chi'(T)]$ = 2.55 ± 0.025 K, and H_c = 1300 ± 50 Oe. In addition, T_c was also determined from the maximum in $d(\chi T)/dT$ to be 2.10 ± 0.05 K, as this is a more accurate determination of T_c for an antiferromagnet.[19] This value correlates well with 2.35 ± 0.05 K.[14b] Polycrystalline samples were used to be consistent with those used in the pressure cell.

The 500 Oe $M(T)$ has a cusp at 2.42 ± 0.05 K at ambient pressure, in accord with antiferromagnetic ordering (Figure 6). The low-temperature magnetization decreases with increasing applied pressure, and the temperature at which the $\chi(T)$ displays a sharp maximum, or cusp, increases to 3.11 ± 0.05 K

dx.doi.org/10.1021/ic302420s | Inorg. Chem. 2013, 52, 1108−1112

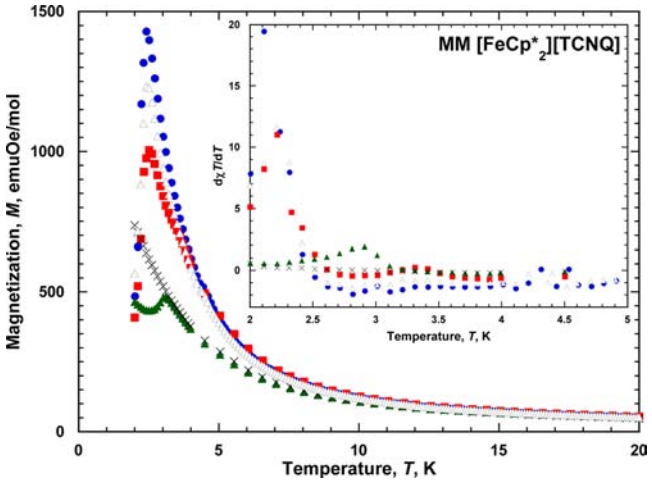

Figure 6. $M(T)$ at 500 Oe for **MM** as a function of pressure: 0.001 (●), 1.3 (■), 2.9 (▲), and 3.9 kbar (×), and upon returning to ambient pressure [0.001 kbar (△)]. Inset is $d(\chi T)/dT$ (note: for ≥3.9 kbar, the $d(\chi T)/dT$ plots are coincident).

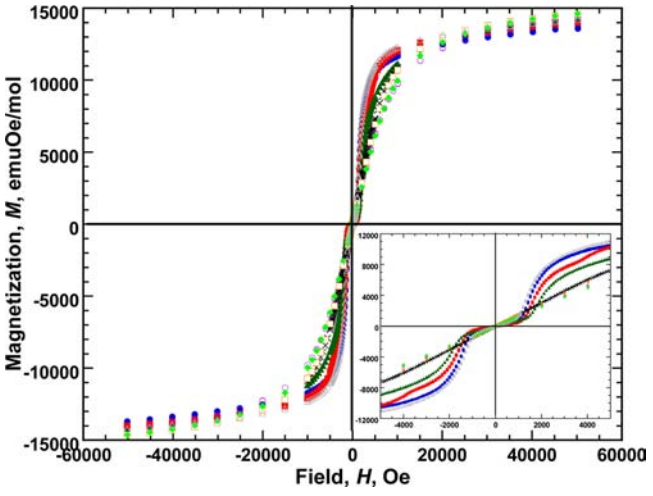

Figure 7. K $M(H)$ of **MM** at ambient pressure, 0.001 (●), 1.3 (■), 2.9 (▲), 3.9 (×), 4.8 (○), 6.6 (□), and 9.2 kbar (♦), and upon returning to ambient pressure [0.001 kbar (△)]. Inset is an expansion about the critical fields: at 1.3 kbar, an incomplete spin flop, as previously reported for eicosane-aligned samples, is evident.[14]

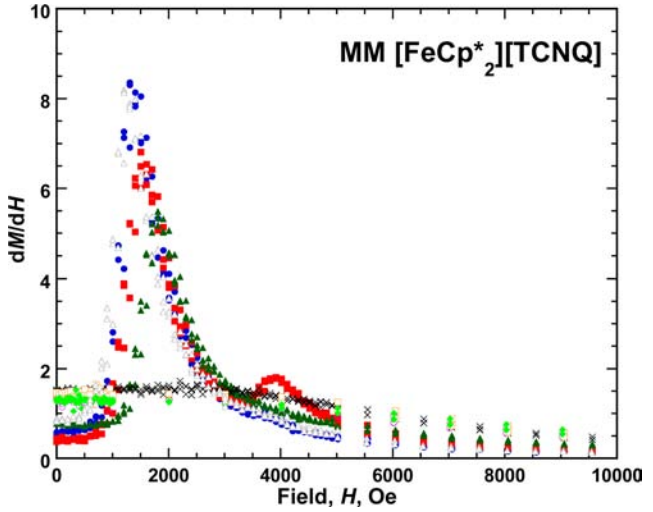

Figure 8. dM/dH of **MM** at several applied pressures: 0.001 (●), 1.3 (■), 2.9 (▲), 3.9 (×), 4.8 (○), 6.6 (□), and 9.2 kbar (♦), and upon returning to ambient pressure [0.001 kbar (△)].

at 2.9 kbar. The T_c for an antiferromagnet is best determined from $d(\chi T)/dT$)[19] (Figures 3 and 6, inset) and is 2.10 ± 0.05 K at ambient pressure, and increases linearly to 2.90 ± 0.05 K at 2.9 kbar, and then abruptly decreases, consistent with a paramagnetic phase transition (Figures 3 and 6, inset).

The magnetization is suppressed with increasing pressure, and this results in a significant decrease of the magnitude for the maximum in the $d(\chi T)/dT$ with increasing pressure (<3.9 kbar), which is evidence of decreasing magnetization, as occurs for **FO** (vide supra), $[FeCp_2^*][TCNE]$,[16] $[FeCp_2^*]^+[DCNQ]^-$,[17] $Fe(pyrimidine)_2Cl_2$,[22] and $MnNi(NO_2)_4$(ethylene-diamine)$_2$.[23] The T_c increases by 0.28 K/kbar below 2.9 kbar (Figure 3), which is consistent with the rate observed in $[FeCp_2^*]^+[TCNE]^-$ (0.22 K/kbar), reaching a maximum of 2.90 ± 0.05 K at 2.9 kbar,[16] and 0.33 K/kbar for $[FeCp_2^*]^+[DCNQ]^-$.[17]

The magnetization for **MM** increased by 6% from 13 700 Oe at ambient pressure to 14 600 Oe at 9.2 kbar at 50 kOe, which is in contrast to **FO** (Figure 7). The "S"-shaped $M(H)$ characteristic of metamagnetic behavior[24] is observed up to 3.9 kbar applied pressure, and a linear Brillouin-like $M(H)$ characteristic of paramagnetic behavior is observed at and above 3.9 kbar. The H_c determined from the maximum in dM/dH (Figure 8) increases linearly from 1300 ± 50 Oe at ambient pressure to 1800 ± 50 Oe at 2.9 kbar (Figure 9), but is not evident at and above 3.9 kbar. This is consistent with the absence of a maximum in the $d(\chi T)/dT$ value and paramagnetic behavior; hence, a transition to a paramagnetic state occurs at ∼3.9 kbar. The T_c, and H_c were restored to their ambient pressure values: 2.20 ± 0.05 K and 1200 ± 50 Oe, respectively, upon release to ambient pressure, indicating reversibility. The increase in T_c and H_c with applied pressure has also been observed for $[FeCp_2^*]^+[DCNQ]^-$,[17] and $Mn^{II}(hfac)_2$(BBA) (hfac = hexafluoroacetylacetonate; BBA = 1,3-bis[*N*-*t*-butylaminoxyl).[25]

Under hydrostatic pressure, the intra- and interchain separations contract, leading to stronger couplings enhancing T_c and the metamagnetic critical field, H_c. However, above 2.9 kbar, a phase transition occurs, leading to paramagnetic behavior. This differs from $Mn^{II}(TCNE)[C_4(CN)_8]_{1/2}\cdot zCH_2Cl_2$ that exhibits a reversible pressure-induced piezomagnetic transition from an antiferromagnetic to a ferrimagnetic state above 0.50 kbar.[26] A study of the pressure-dependent structure is needed to understand the genesis of these effects.

■ CONCLUSION

Temperature- and field-dependent magnetic studies of the **FO** and **MM** polymorphs of $[FeCp^*_2][TCNQ]$ at several applied pressures revealed similar enhancements to the $T_c(M_r(T))$ for ferromagnetic **FO** and $T_c[d(\chi T)/dT]$ for metamagnetic **MM** with an antiferromagnetic ground state, respectively, as the pressure was increased. The enhancement rates of 0.21 and 0.28 K/kbar, respectively, are similar to that of the structurally related electron-transfer salt $[FeCp_2^*]^+[TCNE]^-$, which displayed an enhancement of 0.22 K/kbar $T_c(\chi')$.[16] **FO** was determined to exhibit no H_{cr} at ambient pressure, but H_{cr} and $M_r(H)$ increase to 550 Oe and 8880 emu·Oe/mol at 2 K and 10.3 kbar. **MM** exhibits a linear increase of H_c with pressure,

dx.doi.org/10.1021/ic302420s | *Inorg. Chem.* 2013, 52, 1108−1112

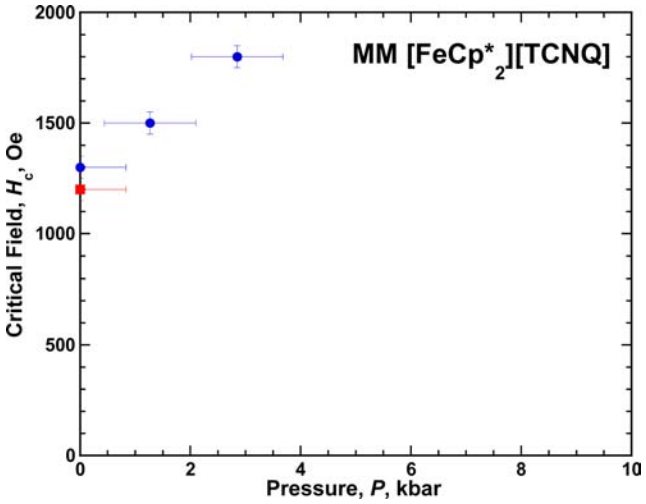

Figure 9. H_c (●) of **MM** for several applied pressures [released pressure (■)].

reaching 1800 Oe at 2.9 kbar. Both the H_c and the T_c are absent at and above 3.9 kbar for the **MM** polymorph, indicative of a pressure-induced transition to a paramagnet. Studies of the pressure-dependent structures are needed to understand the genesis of these effects.

AUTHOR INFORMATION

Corresponding Author

*E-mail: jsmiller@chem.utah.edu.

Notes

The authors declare no competing financial interest.

ACKNOWLEDGMENTS

We appreciate Royce A. Davidson for his assistance with diamagnetic corrections due to the excessive mass of the BeCu pressure apparatus, and the continued support by the U.S. Department of Energy, Basic Energy Sciences, Materials Sciences and Engineering Division (work at University of Utah under contract no. DE-FG03-93ER45504).

REFERENCES

(1) Miller, J. S.; Reis, A. H., Jr.; Gebert, E.; Ritsko, J. J.; Salaneck, W. R.; Kovnat, L.; Cape, T. W.; Van Duyne, R. P. *J. Am. Chem. Soc.* **1979**, *101*, 7111.
(2) Candela, G. A.; Swartzendruber, L. J.; Miller, J. S.; Rice, M. J. *J. Am. Chem. Soc.* **1979**, *101*, 2755.
(3) Miller, J. S.; Calabrese, J. C.; Epstein, A. J.; Bigelow, R. W.; Zhang, J. H.; Reiff, W. M. *J. Chem. Soc., Chem. Commun.* **1986**, 1026.
(4) Miller, J. S.; Calabrese, J. C.; Rommelmann, H.; Chittipeddi, S. R.; Zhang, J. H.; Reiff, W. M.; Epstein, A. J. *J. Am. Chem. Soc.* **1987**, *109*, 769.
(5) Miller, J. S. *J. Mater. Chem.* **2010**, *20*, 1846.
(6) Miller, J. S.; Epstein, A. J.; Reiff, W. M. *Science* **1988**, *240*, 40.
(7) Miller, J. S. *Polyhedron* **2009**, *28*, 1596.
(8) (a) Blundell, S. J.; Pratt, F. L. *J. Phys.: Condens. Matter* **2004**, *16*, R771. (b) Ovcharenko, V. I.; Sagdeev, R. Z. *Russ. Chem. Rev.* **1999**, *68*, 345. (c) Kinoshita, M. *Philos. Trans. R. Soc., A* **1999**, *357*, 2855. (d) Miller, J. S.; Epstein, A. J. *Chem. Commun.* **1998**, 1319. (e) Miller, J. S.; Epstein, A. J. *Angew. Chem., Int. Ed. Engl.* **1994**, *33*, 385. (f) Miller, J. S. *Chem. Soc. Rev.* **2011**, *40*, 3266.
(9) Reis, H.; Preston, L. D.; Williams, J. M.; Peterson, S. W.; Miller, J. S. *J. Am. Chem. Soc.* **1979**, *101*, 2756.
(10) Miller, J. S.; Zhang, J. H.; Reiff, W. M.; Dixon, D. A.; Preston, L. D.; Reis, A. H., Jr.; Gerbert, E.; Extine, M.; Troup, J.; Ward, M. D. *J. Phys. Chem.* **1987**, *91*, 4344.
(11) Broderick, W. E.; Eichhorn, D. M.; Liu, X.; Toscano, P. J.; Owens, S. M.; Hoffman, B. M. *J. Am. Chem. Soc.* **1995**, *117*, 3641.
(12) Her, J.-H.; Stephens, P. W.; Ribas-Ariño, J.; Novoa, J. J.; Shum, W. W.; Miller, J. S. *Inorg. Chem.* **2009**, *48*, 3296.
(13) Chittipeddi, S.; Cromack, K. R.; Miller, J. S.; Epstein, A. J. *Phys. Rev. Lett.* **1987**, *58*, 2695.
(14) (a) Taliaferro, M. L.; Palacio, F.; Miller, J. S. *J. Mater. Chem.* **2006**, *16*, 2677. (b) T_c from the maximum in $d(\chi T)/dT$ for the data reported in reference 14a.
(15) Upon further detailed investigation, **FO** does not exhibit hysteresis, as initially reported.[11]
(16) Huang, Z. J.; Chen, F.; Ren, Y. T.; Xue, Y. Y.; Chu, C. W.; Miller, J. S. *J. Appl. Phys.* **1993**, *10*, 6563.
(17) Hamlin, J. J.; Beckett, B. R.; Tomita, T.; Schilling, J. S.; Tyree, W. S.; Yee, G. T. *Polyhedron* **2003**, *22*, 2249.
(18) Shum, W. W.; Her, J.-H.; Stephens, P. W.; Lee, Y.; Miller, J. S. *Adv. Mater.* **2007**, *19*, 2910.
(19) Fisher, M. E. *Philos. Mag.* **1962**, *7*, 17.
(20) (a) Aharen, T.; Greedan, J. E.; Ning, F.; Imai, T.; Michaelis, V.; Zhou, H.; Wiebe, C. R.; Cranswick, L. M. D. *Phys. Rev. B* **2009**, *80*, 134423. (b) Cage, B.; Nguyen, B.; Dalal, N. *Solid State Commun.* **2001**, *119*, 597.
(21) Carlin, R. L. *Magnetochemistry*; Springer: New York, 1986; pp 202−206.
(22) Wolter, A. U. B.; Klauss, H.-H.; Litterst, F. J.; Burghardt, T.; Eichler, A.; Feyerherm, R.; Süllow, S. *Polyhedron* **2003**, *22*, 2139.
(23) Kreitlow, J.; Mathonière, C.; Feyerherm, R.; Süllow, S. *Polyhedron* **2005**, *24*, 2413.
(24) Stryjewski, E.; Giordano, N. *Adv. Phys.* **1977**, *26*, 487.
(25) Hosokoshi, Y.; Suzuki, K.; Inoue, K.; Iwamura, H. *Mol. Cryst. Liq. Cryst.* **1999**, *334*, 511.
(26) McConnell, A. C.; Bell, J. D.; Miller, J. S. *Inorg. Chem.* **2012**, *51*, 9978.